2023 IEEE Conference on Control Technology and Applications (CCTA)
August 16-18, 2023. Bridgetown, Barbados

Source Localization in Linear Dynamical Systems using Subspace Model Identification

Rajasekhar Anguluri, Nima Taghipourbazargani, Oliver Kosut, and Lalitha Sankar

2023 IEEE Conference on Control Technology and Applications (CCTA) | 979-8-3503-3544-6/23/$31.00 ©2023 IEEE | DOI: 10.1109/CCTA54093.2023.10252510

***Abstract*— We study the problem of localizing sources of unknown forced inputs in linear dynamical systems with unknown system matrices. This problem is relevant in several real-world dynamical systems, including power networks and mechanical systems, where the unknown inputs could be forced oscillations or malicious attacks. Localizing sources is key to mitigating the impact of these unwanted inputs on the system's performance. To this aim, we develop an algorithm that finds sources based on the modal information in the inputs. We obtain this information from the eigenvalues of the (sampled) system matrices, which we estimate using a subspace identification method. Importantly, our algorithm relies on a key assumption that inputs can be appropriately modeled as outputs of some latent linear systems. This assumption allows us to go beyond periodic inputs that are a mainstay in the literature of source localization problems. We illustrate our findings via multiple numerical studies.**

I. Introduction

Real-world engineered systems are often subject to multiple types of disturbances. If the disturbance is small enough and does not trigger the natural modes of the system, then feedback controllers are robust enough to ensure the system's stability or operate near the equilibrium point. However, certain disturbances, such as the harmonic disturbances injected by malfunctioned controllers, malicious inputs injected by adversaries, or cyclic errors in sensors, might not be small in magnitude. In such scenarios, feedback controllers in the system may not be sufficient to protect against the impact of these disturbances, thus requiring disturbance mitigation using other techniques.

A simple and practical method to mitigate the disturbances (henceforth referred to as forced inputs) is to find the location of the sources injecting these inputs and disconnecting them. This method is known as *source localization* [1], [2], [3], [4]. Detecting unknown inputs using measurements is straightforward if the input is present for sufficiently long enough. Several methods exist in the literature discussing various kinds of detection algorithms (see [5] and the cited references). In contrast, localizing sources is a difficult problem because we need to determine the true sources using measurements, with or without the knowledge of the system model.

On the one hand, when the system model is known, the source localization problem can be cast as an unknown input reconstruction problem (also referred to as input deconvolution or forced input reconstruction, [6], [7]). Additionally, if the sources are sparse (i.e., among all possible sources only a few sources inject inputs), we then can find the locations of the true sources using sparsity-constrained unknown batch or sequential estimators; see, for sample, [8], [9], [10]. On the other hand, when the system model is known to belong to a certain model class (e.g., linear or affine systems) with unknown parameters, sources are localized using Discrete Fourier Transform (DFT) methods [2], [11], [12].

While system operators prefer DFT methods coupled with spectral peak-picking and thresholding, these methods have many disadvantages. First, DFT analysis is sensitive to spectral leakage and sensor noise, and hence, the resulting localization algorithms are inefficient. Second, DFT methods are not convenient for estimating system parameters, such as system matrices of linear dynamical systems. These matrices, for instance, help develop signal filters for input cancellation. However, identification methods based on state space models provide a better numerical alternative to DFT methods, both for model identification and source localization [13].

Assuming a latent model for inputs, we develop a state-space model-based subspace identification method to localize the sources using measurements. We employ a state-space model for developing the method, but we do not assume the parameters of the state-space model. Thus, our identification method falls under the category of model-based data-driven methods and is useful where one needs to localize the sources and estimate system models. Further, the subspace method provides appropriate observability and minimality conditions necessary to estimate the system matrices. Consequently, we can use these conditions to enforce observability by adding more sensors if needed.

We summarize our key contributions below.

(i) For a continuous-time linear dyamical system with n states and m inputs, we model each input as an output of a zero-input latent linear dynamical system with one output and an arbitrary number of latent states. This model allows us to capture a large class of external disturbances injected into physical systems.

(ii) Under the above assumptions, we propose a deterministic subspace model identification method to jointly estimate the matrices of the (sampled) linear system and also the sources of the locations (that is, the inputs with non-zero entries). Our method involves solving a simple least squares problem using data collected over a time horizon. We also formally state conditions under which our method correctly identifies the sources.

(iii) We validate the performance of our identification algorithm on a benchmark power system for two cases: purely sinusoidal inputs and non-sinusoidal inputs.

This work is funded in part by the NSF under grant Grant No. OAC-1934766, PSERC project S-87, and Mistletoe Fellowship Award. The authors are affliated with the School of Electrical, Computer and Energy Engineering, Arizona State University, Tempe, AZ 85281, USA (e-mail:{rangulur,ntaghip1,lalithasankar,okosut}@asu.edu).

The rest of the paper is organized as follows. In Section II, we introduce the system model. In Section III, we present the subspace identification method and propose an algorithm to localize the sources in Section IV. In Section V, we provide simulation results. In Section VI, we summarize our paper with future directions.

II. System dynamics under forced Inputs

Consider the continuous linear time-invariant system excited by unknown external forced inputs:

$$\begin{aligned}\dot{\mathbf{x}}(t) &= \mathbf{A}_c\mathbf{x}(t) + \sum_{i=1}^{m}\mathbf{b}_i u_i(t),\\ \mathbf{y}(t) &= \mathbf{C}_c\mathbf{x}(t), \quad \forall t \geq 0,\end{aligned} \tag{1}$$

where $\mathbf{x}(t) \in \mathbb{R}^n$ is the state vector and $\mathbf{y}(t) \in \mathbb{R}^p$ is the output vector. The system is parametrized by matrices $\mathbf{A}_c \in \mathbb{R}^{n\times n}$ and $\mathbf{C}_c \in \mathbb{R}^{n\times p}$, and vectors $\mathbf{b}_i \in \mathbb{R}^n$ for all $i \in \{1,\ldots,m\}$. In (1), without loss of generality, we set the known inputs to zero. We give concrete examples of real-world systems described by (1) in the simulations section.

We assume that the scalar input $u_i(t)$ injected by the i-th source is given as the output of the following latent system:

$$\dot{\mathbf{z}}_i(t) = \mathbf{A}_i\mathbf{z}_i(t) \quad \text{and} \quad u_i(t) = \mathbf{p}_i^{\mathsf{T}}\mathbf{z}_i(t), \tag{2}$$

where $\mathbf{A}_i \in \mathbb{R}^{n_i\times n_i}$ and $\mathbf{p}_i \in \mathbb{R}^{n_i}$, and $\mathbf{z}_i \in \mathbb{R}^{n_i}$ is the latent state. From (2), note that $u_i(t) = \mathbf{p}_i^{\mathsf{T}}\exp(\mathbf{A}_i t)\mathbf{z}_i(0)$. So $u_i(t)$ is completely determined by the tuple $(\mathbf{A}_i, \mathbf{z}_i(0), \mathbf{p}_i)$. In Example 1, we construct a tuple $(\mathbf{A}_i, \mathbf{z}_i(0), \mathbf{p}_i)$ whose system's response can be used to generate sinusoidal inputs.. Finally, except for $\mathbf{y}(t)$, we assume no knowledge of the state vectors, and system matrices and vectors.

Example 1: ***(Sinusoidal Inputs [14])*** Let r be a positive integer. Define $\mathbf{p}_1 = \begin{bmatrix}1 & 0 & 1 & 0 & \ldots & 1 & 0\end{bmatrix}^{\mathsf{T}} \in \mathbb{R}^{2r}$ and the latent state vector with alternating sine and cosine terms:

$$\mathbf{z}_1(t) \triangleq \begin{bmatrix} a_1\sin(w_1 t+\phi_1)\\ a_1\cos(w_1 t+\phi_1)\\ \vdots \\ a_r\sin(w_r t+\phi_r)\\ a_r\cos(w_r t+\phi_r)\end{bmatrix} \in \mathbb{R}^{2r}. \tag{3}$$

Finally, we define $\mathbf{A}_1$ as follows:

$$\mathbf{A}_1 = \begin{bmatrix} \begin{bmatrix}0 & w_1\\ -w_1 & 0\end{bmatrix} & & \\ & \ddots & \\ & & \begin{bmatrix}0 & w_r\\ -w_r & 0\end{bmatrix}\end{bmatrix}. \tag{4}$$

Then $u_1(t) \triangleq \sum_{i=1}^{r} a_i\sin(w_i t+\phi_i)$ can also be obtained using the formula $\mathbf{p}_1^{\mathsf{T}}\exp(\mathbf{A}_1 t)\mathbf{z}_1(0)$. This is because $\dot{\mathbf{z}}_1(t) = \mathbf{A}_1\mathbf{z}_1(t)$, for $\mathbf{A}_1$ and $\mathbf{z}_1(t)$ in (3) and (4) ■

The latent linear system in Example 1 produces a periodic signal with r sinusoidal components. Interestingly, even for $r = 1$, we need a two-dimensional latent state vector (see (3). However, to model external forced inputs beyond decaying or sustained sinusoids, we should consider arbitrary $(\mathbf{A}_i, \mathbf{z}_i(0), \mathbf{p}_i)$. We explore these inputs in simulations.

Using the actual system in (1) and latent systems in (2), we consider the following augmented linear system:

$$\begin{bmatrix}\dot{\mathbf{x}}(t)\\ \dot{\mathbf{z}}_1(t)\\ \vdots\\ \dot{\mathbf{z}}_m(t)\end{bmatrix} = \underbrace{\begin{bmatrix}\mathbf{A}_c & \mathbf{b}_1\mathbf{p}_1^{\mathsf{T}} & \ldots & \mathbf{b}_m\mathbf{p}_m^{\mathsf{T}}\\ \mathbf{0} & \mathbf{A}_1 & \ldots & \mathbf{0}\\ \vdots & \vdots & \ddots & \vdots\\ \mathbf{0} & \mathbf{0} & \ldots & \mathbf{A}_m\end{bmatrix}}_{\mathbf{A}_{\text{full}}}\underbrace{\begin{bmatrix}\mathbf{x}(t)\\ \mathbf{z}_1(t)\\ \vdots\\ \mathbf{z}_m(t)\end{bmatrix}}_{\mathbf{x}_{\text{full}}(t)}, \tag{5}$$

$$\mathbf{y}(t) = \mathbf{C}\mathbf{x}_{\text{full}}(t), \tag{6}$$

where $\mathbf{C} = [\mathbf{C}_c, \mathbf{0}, \ldots, \mathbf{0}]$. If $u_i(t) = \mathbf{p}_i^{\mathsf{T}}(t)\mathbf{z}_i(t) \neq 0$, the i-th source is active. Otherwise, the source is not active.

We assume that sensors record measurements at discrete time instants. Thus, we sample (1) with the sampling period T. Let $\mathbf{A}_d = \exp(\mathbf{A}_{\text{full}}T)$; then $\mathbf{A}_d \in \mathbb{R}^{\tilde{n}\times\tilde{n}}$ with $\tilde{n} = n + n_1 + \ldots + n_m$, where n is the dimension of $\mathbf{x}(t)$ and n_i is the dimension of $\mathbf{z}_i(t)$. Define $\mathbf{x}_d[k] \triangleq \mathbf{x}_{\text{full}}(kT)$ and $\mathbf{y}[k] \triangleq \mathbf{y}(kT)$, where $k = 0, 1, \ldots$. Then

$$\mathbf{x}_d[k+1] = \mathbf{A}_d\mathbf{x}_d[k] \quad \text{and} \quad \mathbf{y}[k] = \mathbf{C}\mathbf{x}_d[k] \tag{7}$$

describe the sampled model of (1).

The goal of source localization problem is to find indices of $u_i[k] \triangleq u_i(kT) \neq 0$ from $\mathbf{y}[k]$, collected over a time window. However, in (7), $u_i[k]$, for every $i \in \{1,\ldots,m\}$ is implicitly defined through the unknown state $\mathbf{x}_d[k]$ and the augmented matrix $\mathbf{A}_d$. In what follows we show that the non-zero input sources can be identified using the eigenvalues of $\mathbf{A}_d$. In Section III we describe a procedure to estimate eigenvalues. Suppose that the system in (5) and (6) is minimal (i.e. if there are no pole-zero cancellations). Then the eigenvalues of $\mathbf{A}_d$ can be obtained using the map $\lambda \to e^{\lambda T}$, where λ is the eigenvalue of $\mathbf{A}_c$. The assumption below states that knowing eigenvalues is equivalent to knowing the sources.

Assumption 2.1: Let spec$(\cdot)$ be the set of eigenvalues.

(i) spec$(\mathbf{A}_i)$ is known and the system in (2) is minimal.
(ii) spec$(\mathbf{A}_c) \cap$ spec$(\mathbf{A}_i) \cap$ spec$(\mathbf{A}_j) = \phi$ for any $i, j \in \{1,\ldots,m\}$ where $i \neq j$. ■

Assumption 2.1(i) is justified by the fact that the system operator is aware of the modes of the input $u_i(t) = \mathbf{p}_i^{\mathsf{T}}\mathbf{z}(t)$ injected by an internal device (for e.g., controller). Further, the minimality assumption guarantees that the modes of $u_i(t)$ are equivalent to spec$(\mathbf{A}_i)$. This assumption does not imply that the system operator knows the sources of the active inputs. Rather this assumption implies that the system operator can identify the source of the input (e.g., malfunctioned or corrupted device) once the modal information is obtained.

Assumption 2.1(ii) is a necessary identifiability condition for localizing the sources using the eigenvalues. Specifically, if Assumption 2.1(ii) is violated, we cannot localize active sources using eigenvalues. Finally, we emphasize that we do not assume any knowledge of $(\mathbf{A}_c, \mathbf{C}_c)$. Thus, our method can localize sources in systems with unknown matrices.

III. Subspace Model Identification

In this section, we develop results on state-space subspace model identification for the deterministic sampled system in (7). This material is fairly standard and our exposition is based on [15], [16]. We then use these results to develop an algorithm to identify the source locations in Section IV.

By invoking (7), we can establish the following mapping between the state $\mathbf{x}_d[k]$ and the measurements $\{\mathbf{y}[k]\}_{k=0}^{s-1}$:

$$\begin{bmatrix} \mathbf{y}[k] \\ \mathbf{y}[k+1] \\ \vdots \\ \mathbf{y}[k+s-1] \end{bmatrix} = \underbrace{\begin{bmatrix} \mathbf{C} \\ \mathbf{C}\mathbf{A}_d \\ \vdots \\ \mathbf{C}\mathbf{A}_d^{s-1} \end{bmatrix}}_{\triangleq \mathcal{O}_s} \mathbf{x}_d[k]. \tag{8}$$

Let $\tilde{n} < s \ll N$, where $\tilde{n} = n + n_1 + \ldots + n_m$ is the dimension of $\mathbf{A}_d$ in (7). Consider the following block Hankel Matrix constructed using $\{\mathbf{y}[k]\}_{k=0}^{N-1}$:

$$\mathbf{Y}_{o,s,N} = \begin{bmatrix} \mathbf{y}[0] & \mathbf{y}[1] & \ldots & \mathbf{y}[N-s] \\ \mathbf{y}[1] & \mathbf{y}[2] & \ldots & \mathbf{y}[N-s+1] \\ \vdots & \vdots & \ddots & \vdots \\ \mathbf{y}[s-1] & \mathbf{y}[s] & \ldots & \mathbf{y}[N-1] \end{bmatrix}. \tag{9}$$

Substituting the relation (8) in (9) for different time shifts, yields the following data equation:

$$\mathbf{Y}_{o,s,N} = \mathcal{O}_s \underbrace{\begin{bmatrix} \mathbf{x}_d[0] & \mathbf{x}_d[1] & \ldots & \mathbf{x}_d[N-s] \end{bmatrix}}_{\triangleq \mathbf{X}_{0,N}}. \tag{10}$$

The essence of subspace identification methods is estimating system matrices using the Hankel matrix in (9) using factorizations similar to the one described in (10). In our case, to estimate $(\mathbf{A}_d, \mathbf{C}_c)$ using $\mathbf{Y}_{o,s,N}$, we begin with the following assumption:

Assumption 3.1: $\text{rank}(\mathbf{X}_{0,N}) = \tilde{n}$ and $\text{rank}(\mathcal{O}_s) = \tilde{n}$. ■

Assumption 3.1 ensures that the rank of $\mathbf{Y}_{o,s,N}$ equals $\tilde{n}$. Thus, $\text{range}(\mathbf{Y}_{o,s,N}) = \text{range}(\mathcal{O}_s)$ (here $\text{range}(\cdot)$ means the column space of the matrix). This identity allows us to use the left singular vectors of $\mathbf{Y}_{o,s,N}$ as basis vectors for $\mathcal{O}_s$ to estimate $(\mathbf{A}_d, \mathbf{C})$ up to an unknown similarity transformation matrix $\mathbf{T}$. We give high-level details of this method below. For a leisurely derivation, we refer the reader to see [16].

Consider the following SVD of $\mathbf{Y}_{o,s,N}$:

$$\mathbf{Y}_{o,s,N} = \left[\begin{array}{c|c} \mathbf{U}_{\tilde{n}} & \mathbf{U}_{\text{noise}} \end{array}\right] \left[\begin{array}{c|c} \mathbf{\Sigma}_{\tilde{n}} & \mathbf{0} \\ \hline \mathbf{0} & \mathbf{\Sigma}_{\text{noise}} \end{array}\right] \left[\begin{array}{c} \mathbf{V}_{\tilde{n}}^{\mathsf{T}} \\ \hline \mathbf{V}_{\text{noise}}^{\mathsf{T}} \end{array}\right] \tag{11}$$

with $\mathbf{\Sigma}_{\tilde{n}} \in \mathbb{R}^{\tilde{n}\times\tilde{n}}$, $\text{rank}(\mathbf{\Sigma}_{\tilde{n}}) = \tilde{n}$, and $\mathbf{\Sigma}_{\text{noise}} = \mathbf{0}$ (follows from the fact that the rank of $\mathbf{Y}_{o,s,N} = \tilde{n}$ and that there is no noise). Because the column spaces of $\mathbf{Y}_{o,s,N}$ and $\mathcal{O}_s$ are equal, there exist a matrix $\mathbf{T}$ such that $\mathbf{U}_{\tilde{n}}\mathbf{T}^{-1} = \mathcal{O}_s$. Thus,

$$\mathbf{U}_{\tilde{n}} = \mathcal{O}_s\mathbf{T} = \begin{bmatrix} \mathbf{C}\mathbf{T} \\ \mathbf{C}\mathbf{T}(\mathbf{T}^{-1}\mathbf{A}_d\mathbf{T}) \\ \vdots \\ \mathbf{C}\mathbf{T}(\mathbf{T}^{-1}\mathbf{A}_d\mathbf{T})^{s-1} \end{bmatrix} = \begin{bmatrix} \mathbf{C}_{\mathbf{T}} \\ \mathbf{C}_{\mathbf{T}}\mathbf{A}_T \\ \vdots \\ \mathbf{C}_{\mathbf{T}}\mathbf{A}_T^{s-1} \end{bmatrix}, \tag{12}$$

where $\mathbf{C}_T = \mathbf{C}\mathbf{T}$ and $\mathbf{A}_T = \mathbf{T}^{-1}\mathbf{A}_d\mathbf{T}$. The second equality follows by substituting $\mathcal{O}_s$ defined in (8). Finally, note that $\mathbf{T}$ is nonunique.

From (12), we note that $\mathbf{C}_T$ is given by the first p rows of $\mathbf{U}_{\tilde{n}}$; that is, $\mathbf{C}_T = \mathbf{U}_{\tilde{n}}(1:p,:)$ (we follow the convention of MATLAB to denote rows and columns). The matrix $\mathbf{A}_T$ can be estimated using the shifting property of $\mathcal{O}_s$. Indeed, note the following identity from (12):

$$\mathbf{U}_{\tilde{n}}(1:(s-1)p,:)\mathbf{A}_T = \mathbf{U}_{\tilde{n}}(p+1:sp,:). \tag{13}$$

Because $s > n$, the matrix $\mathbf{A}_T$ can be determined from the overdetermined equations above. We can obtain $\mathbf{A}_T$ as

$$\mathbf{A}_T = (\mathbf{U}_{\tilde{n}}(1:(s-1)p,:))^{+}\mathbf{U}_{\tilde{n}}(p+1:sp,:), \tag{14}$$

where $(\cdot)^{+}$ denotes the Moore-Penrose pseudo inverse.

Because $\mathbf{T}$ is non-unique there exist infinitely many pairs $(\mathbf{A}_T, \mathbf{C}_T)$, parameterized by $\mathbf{T}$, that can describe the dynamics of (7). Specifically, all these pairs give rise to the same measurements. Nonetheless, for any $\mathbf{T}$, the eigenvalues of $\mathbf{A}_d$ and $\mathbf{A}_T$ given in (14) are the same. This is because eigenvalues are invariant under similarity transforms. We use this fact to develop our source localization algorithm.

IV. Source localization via estimated eigenvalues

In this short section, we describe our source localization algorithm using the matrix $\mathbf{A}_T$ in (14).

First, we make a mild technical assumption: let $\lambda = s + j\omega$ and $\rho = s + j\phi$ be any two eigenvalues of $\mathbf{A}_i$ and $\mathbf{A}_k$ in (2), respectively, for all $i, k \in \{1, \ldots, m\}$. Then, ω and ϕ are not integral multiples of $2\pi/T$. This assumption along with Assumption 2.1 (ii) ensures that the eigenvalues $\exp(\lambda T)$ and $\exp(\rho T)$ of $\mathbf{A}_T$ are different. Second, we assume that the augmented system dimension $\tilde{n}$ is known (see below for details on estimating $\tilde{n}$). Third, because $\mathbf{A}_{\text{full}}$ in (5) is block triangular, the eigenvalues of the ith latent system in $\mathbf{A}_d$ in (7) can be obtained as $\exp(\lambda(\mathbf{A}_i)T)$.

With the above observations in place, define the information set $\mathcal{I} = \cup_{i=1}^{m}\mathcal{I}_i$, where $\mathcal{I}_i = \{e^{\lambda_{k_i}(\mathbf{A}_i)}, \ldots, e^{\lambda_{n_i}(\mathbf{A}_i)}\}$. We can now uniquely locate sources using the eigenvalues of $\mathbf{A}_T$. We detail the steps in the joint model identification and source localization method in Algorithm 1.

Algorithm 1: Source localization via measurements.

Input: System order ($\tilde{n}$), integers s and N such that $N > s > \tilde{n}$, measurements $\{\mathbf{Y}[k]\}_{k=0}^{N-1}$, and the set of eigenvalues $\mathcal{I} = \cup_{i=1}^{m}\mathcal{I}_i$.

Step 1: Construct the block Hankel matrix $\mathbf{Y}_{0,s,N}$ in (9) using the measurements $\{\mathbf{Y}[k]\}_{k=0}^{N-1}$.

Step 2: Compute the SVD of $\mathbf{Y}_{0,s,N}$ and obtain $\mathbf{U}_{\tilde{n}}$ as described in (11).

Step 3: Obtain $\mathbf{A}_T$ using (14) and its eigenvalues $\widehat{\lambda}_d$.

Step 4: Flag sets $\mathcal{I}_i$ whose eigenvalues matches with any one of the estimated quantities $\widehat{\lambda}_d$.

Return: Sources corresponding to the eigenvalues $\widehat{\lambda}_c$.

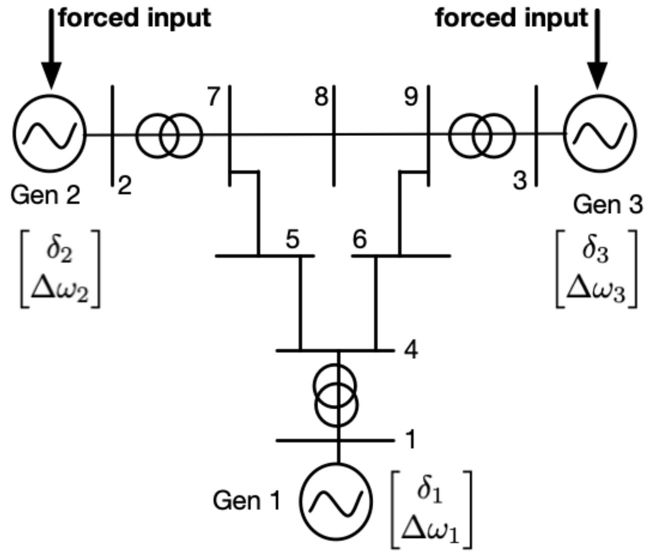

Fig. 1: Three generator, nine bus system [17]. The forced inputs enter the system through Gen2 and Gen3.

V. Simulations

We apply Algorithm 1 to localize sources of forced inputs in a three-generator, nine-bus system shown in Fig. 1. The generators are connected to nine network buses (numbered vertical and horizontal lines in Fig. 1). The i-th generator is associated with two states $(\delta_i, \Delta\omega_i)$, where δ_i is the rotor angle and $\Delta\omega_i$ is the angular frequency, for all $i \in \{1,2,3\}$.

Define $\mathbf{x}(t) = [\delta_1, \delta_2, \delta_3, \Delta\omega_1, \Delta\omega_2, \Delta\omega_3]^\mathsf{T}$. The inputs $u_i(t)$, for all $i \in \{1,2,3\}$, correspond to the power injection deviations at the generators. Applying Kron reduction, we have the following continuous-time state and input matrices describing the evolution of $\mathbf{x}(t)$ [17]:

$$\mathbf{A}_c = \left[\begin{array}{ccc|ccc} 0.000 & 0.000 & 0.000 & 1.000 & 0.000 & 0.000 \\ 0.000 & 0.000 & 0.000 & 0.000 & 1.000 & 0.000 \\ 0.000 & 0.000 & 0.000 & 0.000 & 0.000 & 1.000 \\ \hline -0.341 & -0.043 & -0.059 & -1 & 0 & 0 \\ -0.472 & -2.219 & -1.075 & 0 & -2 & 0 \\ 0.141 & 0.391 & -3.778 & 0 & 0 & -3.692 \end{array}\right]; \text{and}$$

$\mathbf{b}_1 = [0,0,0,8,0,0]^\mathsf{T}$; $\mathbf{b}_2 = [0,0,0,0,29.41,0]^\mathsf{T}$; and $\mathbf{b}_3 = [0,0,0,0,0,76.92]^\mathsf{T}$. From the sparity pattern of $\mathbf{b}_i$, it is clear that $u_i(t)$ directly impacts $\Delta\omega_i(t)$. The sensor matrix is

$$\mathbf{C}_c = \begin{bmatrix} 0 & 0 & 0 & 1 & 0 & 0 \\ 0 & 0 & 0 & 0 & 1 & 0 \end{bmatrix}. \qquad (15)$$

Finally, the measurement horizon is $N = 80$ and the Hankel matrix parameter $s = 20$.

Below we consider three cases with different input signals to highlight the superiority of Algorithm 1. To run Algorithm 1, we need the system dimension $\tilde{n}$ (see Step 3 in Algorithm 1). In light of sensor noise and numerical errors, we employ the *best rank approximation* that is based on the ratio of the singular values of $\mathbf{Y}_{o,s,N}$ to estimate $\tilde{n}$ [15]. We compute $\beta(\tilde{n}') = (\sum_{i=1}^{\tilde{n}'} \sigma_i)/(\sum_{i=1}^{\min\{ps,N\}} \sigma_i)$ for various values of $\tilde{n}'$, starting with $\tilde{n}' = 1$. For a predetermined choice of τ we then select the dimension as the least $\tilde{n}'$ for which $\beta(\tilde{n}') \geq \tau$. In our case, we set $\tau = 0.98$.

A. Case 1: sinusoidal inputs (noisy measurements)

We set $u_1(t) = 0$ and consider $u_2(t) = \sin(3t + \pi/2) + \sin(4t + \pi/13)$ and $u_3(t) = \sin(5t + \pi/5) + \sin(6t + \pi/4)$. We then use the construction in Example 1 to obtain latent system's tuple $(\mathbf{A}_i, \mathbf{p}_i, \mathbf{z}_i(0))$, for $i \in \{2,3\}$. Using $\mathbf{A}_1$, $\mathbf{A}_2$, and $\mathbf{A}_c$ of the power system, we obtain the augmented model in (5) and (6). We then obtain the sampled model in (7) using the sampling period $T = 0.1$ seconds. Finally, $\tilde{n}_1 = \tilde{n}_2 = 4$. So, the true system's dimension is $\tilde{n} = 6 + 4 + 4 = 14$. We add Gaussian noise with standard deviation 0.01 to $\mathbf{Y}_{o,s,N}$. The estimated dimension $\tilde{n}' = 13$ (see Fig. 2 (b)).

In Fig. 2 (c), we compare the eigenvalues of $\widehat{\mathbf{A}}_d$ (computed using Step 3 in Algorithm 1) and the eigenvalues of $\mathbf{A}_d$. Except for one eigenvalue of the power system, the estimated eigenvalues are very close to the true eigenvalues. So, our method accurately localizes the sources.

B. Case 2: arbitrary inputs (noise-free measurements)

We set $u_1(t) = 0$, and generate $u_2(t)$ and $u_3(t)$ using the latent system model in (2). We obtain $\mathbf{A}_i$ using MATLAB's in-built function (rss) so that the latent system has stable dynamics. We choose $\mathbf{p}_i$ and $\mathbf{z}_i(0)$ to be zero-mean Gaussian random vectors. Similar to Case 1, we obtain the sampled model in (7) using $T = 0.1$ seconds. The true system dimension $\tilde{n} = 6 + 4 + 4 = 14$. We consider noise free measurements. Hence, $\tilde{n}' = \tilde{n} = 14$ (see Fig. 3 (b)).

In Fig. 3 (c), we compare the eigenvalues of $\widehat{\mathbf{A}}_d$ and the eigenvalues of $\mathbf{A}_d$. Because there is no measurement noise, the estimated eigenvalues are equal to the true eigenvalues. In this case, as well, we have perfect localization.

C. Case 3: arbitrary inputs (noisy measurements)

We set $u_1(t) = u_2(t) = 0$, and obtain $u_3(t)$ using the model in (2). We follow the same procedure in Case 2 to obtain the sampled model. The system dimension $\tilde{n} = 6 + 4$. We add Gaussian noise with standard deviation 0.01 to $\mathbf{Y}_{o,s,N}$. The estimated dimension $\tilde{n}' = 7$ (see Fig. 4 (c)). Unlike Case 1, the impact of the noise on $\tilde{n}' = 7$ is large.

In Fig. 4 (c), we compare the eigenvalues of $\widehat{\mathbf{A}}_d$ and the eigenvalues of $\mathbf{A}_d$. Because $\tilde{n}'$ is smaller than $\tilde{n}$, it is evident that the we cannot estimate all the eigenvalues. However, as illustrated in Fig. 4 (c), the latent system's eigenvalues are perfectly estimated. So, we have perfect localization in this case too, but with a reduced-order system model.

We provide a possible explanation as to why the estimates of the actual system's eigenvalues are poor in this case. The matrix $\mathbf{A}_d$ is a strictly stable system (all eigenvalues are inside the unit disc). Thus, the states, and ultimately, the measurements converge to zero quickly (compare Fig. 2 (a) and Fig. 3(a)). So even a slight measurement noise distorts the true signal, and leads to spurious eigenvalues (see the isolated red circle in Fig. 4(b)).

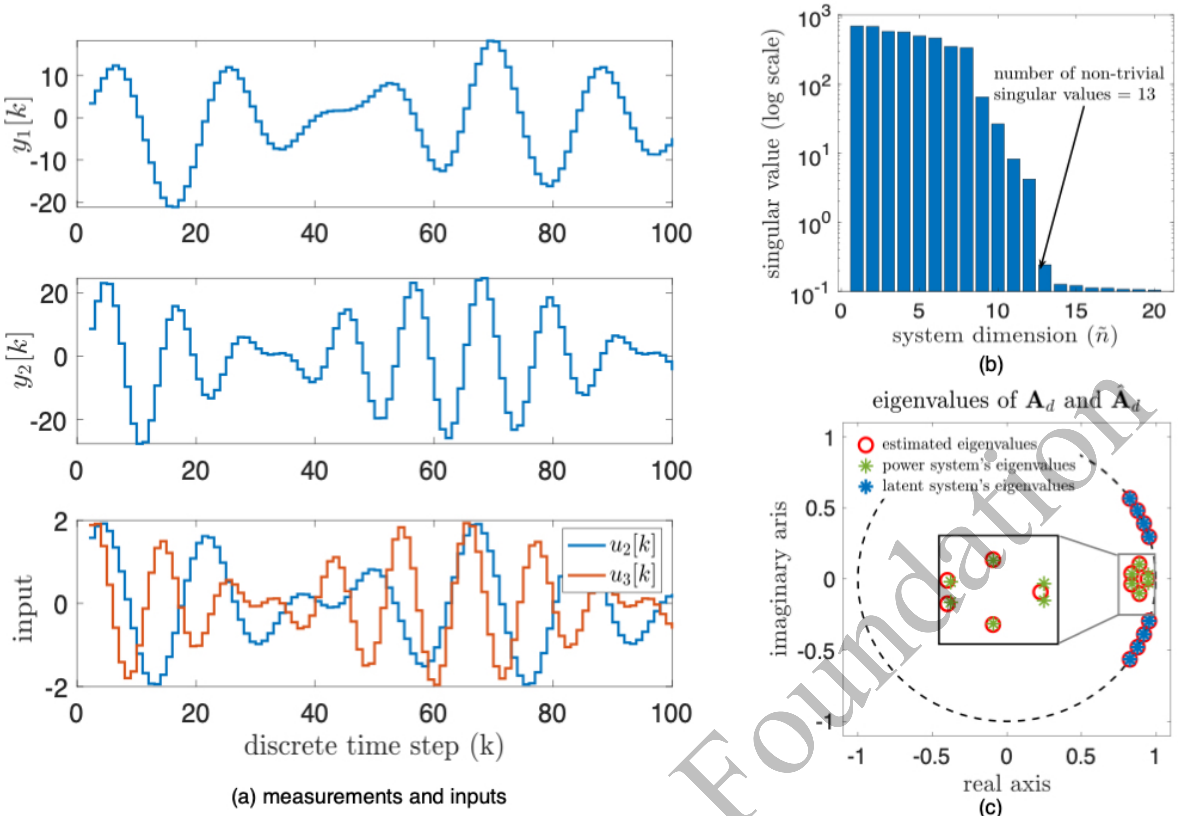

Fig. 2: Source localization with sinusoidal inputs. (a) Noisy frequency measurements recorded by sensors located at Gen1 and Gen2, and inputs are at Gen2 and Gen3. (b) Singular values of the Hankel matrix. (c) Eigenvalues in the complex plane.

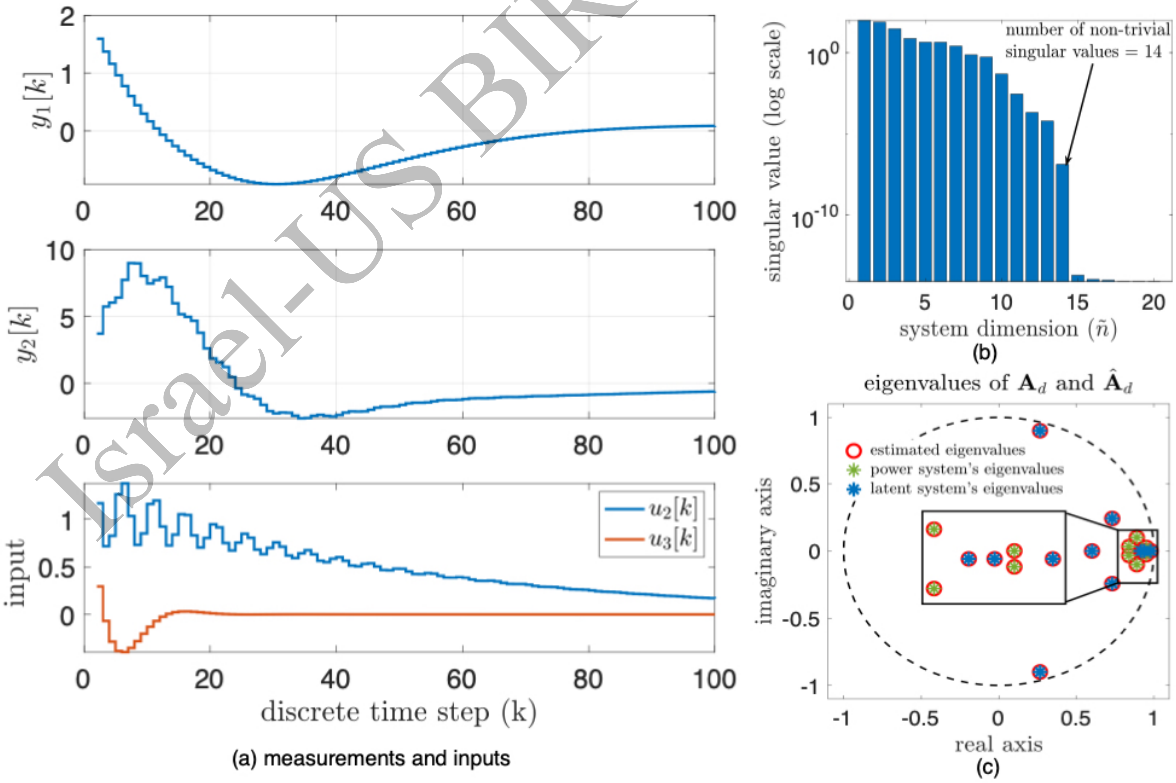

Fig. 3: Source localization with arbitrary inputs. (a) Noise-free frequency measurements recorded by sensors located at Gen 1 and Gen 2, and inputs are at Gen2 and Gen3. (b) Singular values of the Hankel matrix. (c) Eigenvalues in the complex plane.

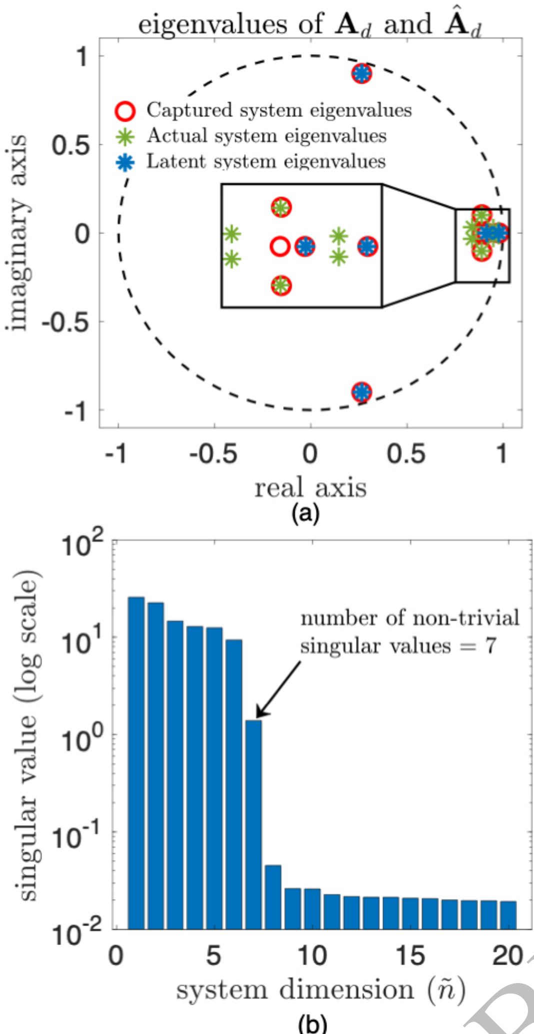

Fig. 4: Source localization with one arbitrary input at Gen3 using noisy measurements. (b) Singular values of the Hankel matrix. (c) Eigenvalues in the complex plane.

VI. Concluding Remarks

We have proposed a subspace model identification method for localizing the sources of forced inputs in unknown linear dynamical systems. Assuming a latent linear model for the forced inputs and a prior knowledge of the input signal's modal content, we cast the source localization problem as estimating the eigenvalues of a certain augmented state-space model. Our joint system identification and source localization Algorithm 1 is simple and has the potential to be integrated into real-time system monitoring operations. We have demonstrated the performance of the proposed method on a benchmark power system for several different input models.

We plan to develop disturbance rejection controllers based on the estimated state-space model for counteracting the forced inputs for future work.

References

[1] S. Roy, W. Ju, N. Nayak, and B. Lesieutre. Localizing power-grid forced oscillations based on harmonic analysis of synchrophasor data. In *55th Annual Conference on Information Sciences and Systems*, pages 1–5, 2021.

[2] R. Anguluri, N. Taghipourbazargani, O. Kosut, and L. Sankar. A complex-LASSO approach for localizing forced oscillations in power systems. In *2022 IEEE Power & Energy Society General Meeting (PESGM)*, pages 01–05, 2022.

[3] W. Feng, Q. Li, and Q. Lu. Force localization and reconstruction based on a novel sparse Kalman filter. *Mechanical Systems and Signal Processing*, 144:106890, 2020.

[4] W. Feng, Q. Li, Q. Lu, C. Li, and B. Wang. Group relevance vector machine for sparse force localization and reconstruction. *Mechanical Systems and Signal Processing*, 161:107900, 2021.

[5] M. Basseville and I. V. Nikiforov. *Detection of abrupt changes: theory and application*, volume 104. prentice Hall Englewood Cliffs, 1993.

[6] J Sanchez and H. Benaroya. Review of force reconstruction techniques. *Journal of Sound and Vibration*, 333(14):2999–3018, 2014.

[7] S. Kirtikar, H. Palanthandalam-Madapusi, E. Zattoni, and D. S. Bernstein. L-delay input and initial-state reconstruction for discrete-time linear systems. *Circuits, Systems, and Signal Processing*, 30:233–262, 2011.

[8] S. Sefati, N. J. Cowan, and R. Vidal. Linear systems with sparse inputs: Observability and input recovery. In *2015 American Control Conference (ACC)*, pages 5251–5257, 2015.

[9] S. M. Fosson, F. Garin, S. Gracy, A. Y. Kibangou, and D. Swart. Input and state estimation exploiting input sparsity. In *2019 18th European Control Conference (ECC)*, pages 2344–2349, 2019.

[10] S. Nagarajaiah. Sparse and low-rank methods in structural system identification and monitoring. *Procedia Engineering*, 199:62–69, 2017.

[11] B. Wang and K. Sun. Location methods of oscillation sources in power systems: a survey. *J. of Modern Power Sys. and Clean Energy*, 5(2):151–159, 2017.

[12] P. Stoica and R. Moses. *Introduction to Spectral Analysis*. Upper Saddle River, NJ: Prentice-Hall, 1997.

[13] J.V. Candy. Subsystem estimation: A modal decomposition approach. Technical report, Lawrence Livermore National Lab.(LLNL), Livermore, CA (United States), 2022.

[14] S. Greś, M. Döhler, P. Andersen, and L. Mevel. Kalman filter-based subspace identification for operational modal analysis under unmeasured periodic excitation. *Mechanical Systems and Signal Processing*, 146:106996, 2021.

[15] J.V. Candy. *Model-based processing: an applied subspace identification approach*. John Wiley and Sons, 2019.

[16] M. Verhaegen and V. Verdult. *Filtering and system identification: a least squares approach*. Cambridge university press, 2007.

[17] S. Nateghi, Y. Shtessel, C. Edwards, and J-P. Barbot. Secure state estimation and attack reconstruction in cyber-physical systems: Sliding mode observer approach. In *Control Theory in Engineering*, page 3. IntechOpen, 2019.